

EFFECT OF GRAPHITE FURNACE DEGRADATION ON ATOMIC ABSORPTION SIGNALS

A. N. Kulik,^{a*} Yu. V. Rogulsky,^a O. M. Buhay,^a
V. Yu. Illiashenko,^b and A. N. Kalinkevich^a

UDC 543.421

The time dynamics of degradation of the working characteristics of longitudinally heated furnaces for spectrometers with electrothermal atomization of a sample in the presence of tungsten, zirconium, and palladium compounds used as chemical modifiers were studied. Visual changes in the state of the investigated furnaces are discussed. The loss of carbon material during the experiment is shown. Atomic absorption signals of silver and copper recorded at different stages of degradation of unmodified and modified furnaces are analyzed. An explanation of the reasons for the accelerated damage to the pyrographite coating and subsequent destruction of the polycrystalline graphite base of furnaces subjected to modification is suggested.

Keywords: *graphite furnaces, pyrolytic graphite, degradation, chemical modifier, atomization.*

Introduction. Atomic absorption spectrometry with electrothermal atomization in a graphite furnace (ETAAS) is one of the most common and available of widely used spectroanalytical methods. The slow pace of ETAAS analysis is compensated by the high sensitivity, low elemental detection limits, reliable and simple instrument construction, and relatively inexpensive analytical equipment.

The time dependence of the heating of a so-called "aged" furnace with a pyrographite coating (PGC) is known to change according to operators with long-term experience working with atomic absorption spectrometry (AAS) combined with electrothermal atomization (ETA) [1–3]. However, this phenomenon was explained by the decreased mass of the furnace and was not thoroughly studied. A furnace loses material to wear unevenly and can overheat in places where the wall cross-sectional area is the smallest [4–7]. This aspect has been discussed before [8]. The difference between the set and actual temperature can adversely affect the accuracy and precision of the measurements.

The wear rate of furnaces depends mainly on the impurity content of the protective gas, the temperature program, the volume and composition of the injected sample, and the used chemical modifiers (CM). The use of CM can increase [9] or decrease the service life of graphite furnaces [1, 3, 7]. CM are classified as permanent modifiers and platinum-group metals, in particular, tungsten (W), zirconium (Zr), and palladium (Pd), according to the mechanism of action. The parameters of the obtained atomization curves should change if they are added to a sample, i.e., the shape of the analytical signal should change and its initial appearance should shift.

Silver (Ag) and copper (Cu) are typical test elements for AAS with ETA in studies of the kinetics, mechanism of atomization, etc. because Ag does not react with graphite and is easily atomized while Cu is held in the furnace-wall pores and has a significantly higher atomization temperature [10]. The spectrometer can be quickly retuned during an experiment because the analytical lines of Ag and Cu are similar.

The goal of the present work was to study the effect of surface degradation in the presence of the selected CM on the appearance, mass, shape, and geometric dimensions of graphite furnaces with PGC and the change of analytical signal parameters of Ag and Cu during wear.

Experimental. The setup for furnace wear consisted of an C115-M1 atomic absorption spectrometer combined with a Grafit-2 electrothermal atomizer (KAS-120.1 system, OAO SELMI, Ukraine). The system was equipped with an

*To whom correspondence should be addressed.

^aInstitute of Applied Physics, National Academy of Sciences of Ukraine, Sumy, 40030, Ukraine; email: cainelexy@gmail.com; ^bSumy State University, Sumy, 40030, Ukraine; email: cainelexy@gmail.com. Translated from Zhurnal Prikladnoi Spektroskopii, Vol. 87, No. 4, pp. 540–547, July–August, 2020. Original article submitted May 5, 2020.

electrothermal atomizer and an analog of a Massman furnace. The operating temperature range was 290–3340 K; heating rate in standard mode up to 2000 K/s; and uncertainty of the temperature program, $\leq 5\%$. The atomizer was water-cooled. A hollow-cathode lamp acted as the source of the characteristic radiation of the measured elements. Effects of nonselective light absorption were eliminated using a deuterium background corrector. Radiation with the resonant wavelength was fed into a photomultiplier. The furnace was purged externally and internally with protective gas (Ar).

Standard furnaces without platforms and analogous to the HGA-500 [length 28 mm, inner and outer diameters 6 and 7.6 mm, sample injection hole (SIH) radius 1 mm; PerkinElmer] made of MPG-6 polycrystalline graphite [electrographite (EG)] with a pyrographite (PG) coating were used. The average furnace mass was ~ 0.9 g. A VLR-20g analytical balance was used for weighing. Calibration solutions of Ag and Cu were prepared using reference standard aqueous solutions of appropriate metal salts (Merck). The analytical lines had $\lambda = 328.1$ and 324.7 nm. The spectral slit width was 0.4 nm.

Modifiers (1 g/L) were prepared by dissolving chemically pure sodium tungstate and zirconyl nitrate in HNO_3 (0.1 M). Pd nitrate solution was prepared by reacting chemically pure metal with HNO_3 . The concentrations of Ag and Cu working solutions were 0.025 and 0.1 mg/L. Solutions were injected into the furnace using an MD-10 syringe to give a sample volume of 10 μL .

The temperature program (cycle) for Ag consisted of drying the liquid at 360–380 K for 60 s, pyrolysis at 770 K with an Ar purge at $2 \cdot 10^{-6}$ m^3/s , atomization at 2070 K for 5 s in stop-flow mode, and annealing of the furnace (~ 3000 K) with flowing protective gas. Cu was pyrolyzed at 1270 K and atomized at 2770 K. The atomization time (measured range) was selected so that the furnace did not overheat. Otherwise, the atomizer was automatically turned off.

The temperature program for measuring Cu and equal total volumes of liquid samples (20 μL) were used for all furnaces during wear. The injections were made in two steps, i.e., 10 μL of modifier-salt solution and 10 μL of blank solution (0.1 M HNO_3). The control furnace was injected twice with blank solution. Periodically, the second injection was replaced by working analyte solution (Ag or Cu) with Ag measured using a separate temperature program. The atomic absorption signal of the analyte was scanned in steps of 0.016 s and stored in a computer. Measured values were further processed by software. The furnace was checked after planned inspections and weighings to ensure it occupied the initial position inside the atomizer.

Results and Discussion. The individual parameters and shapes of the experimental furnace atomizers changed during the degradation process. The samples had a much stronger effect on the graphite loss rate because the temperature program was the same for all furnaces. Zones with possible admission of air, i.e., SIH and gaps between atomizer graphite bushings holding the furnace (electrical contacts), showed the most noticeable destruction. The mechanical action of the syringe was responsible for accelerating wear near the SIH. The wear rates of furnaces without added CM and with added sodium tungstate, zirconyl nitrate, and palladium nitrate differed significantly (Table 1).

Changes became noticeable at ~ 100 cycles in the control furnace, where the sample was blank solution. The outer PGC layer was damaged mainly in the half of the atomizer inserted deeply into the graphite bushing. Impurities captured by the protective gas from the environment reacted more vigorously with the material surface probably because the temperature was elevated by heat transfer from the bushing walls to the inside. Markings opposite to the purge holes remained after 100 heat cycles on the opposite end of the furnace, despite the initially high-purity Ar. Traces of SIH damage were noticeable after ~ 200 cycles. Then, destruction of the furnace only progressed. The PGC burned up. The SIH expanded. Wear was sharply activated after 240 cycles. PGC on the outer side of the furnace surrounded by the graphite bushing was practically gone after ~ 320 cycles. Characteristic gray crystals of sublimed graphite, harbingers of impending furnace failure, appeared in the analytical zone around the noticeably expanded SIH after 380 cycles. The furnace bent (389 cycles) in the analytical zone, where the wear was greatest, because of pressure from the graphite bushings of the holder (Fig. 1).

The CM caused all furnaces to fail for various reasons before extensive loss of the PGC began in the control furnace with identical temperature programs, i.e., other destructive factors apparently associated with the sample chemical composition played a decisive role. For example, addition of sodium tungstate accelerated SIH expansion while other damage was less evident. The destruction was noticeable after 40 cycles and intensified after 100 cycles. The diameters were 3 mm after 140 cycles; 3.5, 160; 4.2, 180; and 5, 200. Interference critical to the measurements soon appeared. A crack in the analytical zone was observed in the next inspection (203 cycles). A characteristic feature of the wear in the presence of the tungstate was that the furnace PGC remained intact for a long time. However, the EG situated between the PG layers was gradually lost. The EG became accessible because the edge of the SIH was worn by the end of the syringe.

Zirconyl nitrate caused the outer PGC of the furnace around the SIH to disappear already after 20 heating cycles, gradually exposing the EG and forming a groove up to 5 mm. However, the SIH was practically not expanded. The outer PGC

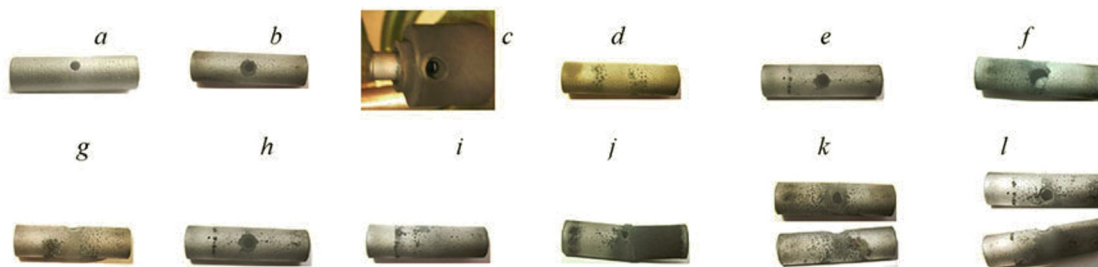
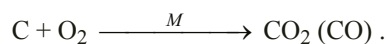


Fig. 1. Visual changes of graphite furnaces due to degradation in the presence of modifiers: new furnace (a), Zr-modified (b, d, g, k), Pd-modified (c, e, h, i, l); W-modified (f); without modifier (j).

was destroyed after 100 cycles along the boundary of the analytical zone, where the main mass of the CM was concentrated during drying of the sample. The centers of the destruction appeared as pits with a light-blue substance within and a bluish color on the edges. Several of the pits became perforations. The furnace failed because the SIH was deformed (189 cycles) regardless of the wall perforations.

Palladium nitrate used as the CM produced the first signs of furnace degradation already after 60 heating cycles. The appearance was clearly changed after 80 cycles. The PGC around the SIH disappeared. Damaged points on the PGC were distinctly concentrated opposite the gap between the atomizer graphite bushings and scattered randomly over the furnace wall predominantly in the part inserted deeply into the bushings. A black substance around the damaged points, essentially emergence of EG pores onto the surface, was probably diffused palladium black [11]. The wear intensified considerably already after 200 cycles, especially of the part inserted into the atomizer graphite bushings. The SIH expanded although less than without modifier. The wall in the furnace analytical zone was critically thinned after 233 cycles. Signs of overheating (sublimed graphite) appeared. Measurements had to be stopped because of interference.

The probable cause of the accelerated degradation of the graphite furnaces in the presence of W, Zr, and Pd CM was their catalytic action during carbon oxidation, in particular, by oxygen held in pores, added with protective gas, contained in H₂O molecules, or incorporated into solid oxides [12–18]. This helped to convert furnace material into volatile carbon oxides that were removed from the atomizer by the stream of protective gas:



The destructive capabilities of the examined CM had their own nuances. Tungsten oxides that were formed via thermal decomposition of the tungstate reacted with the relatively inert PG. Therefore, the furnace was destroyed initially at access sites to the more active EG, e.g., at the SIH. Zr, in contrast to W, could penetrate and concentrate in the graphite wall. Therefore, its damage was observed primarily near the injection point of the zirconyl nitrate [19]. Pd in Pd black could occur in all furnace pores [11]. Therefore, it caused more or less even wear. The furnace mass decreased predictably during degradation. The lack of modifier had a positive effect on the operating lifetime of the furnace. The control furnace failed much later than the others, despite having the smallest mass. The formation of many pits and holes alongside Zr compounds in the analytical zone was indicative of extensive mass loss within the furnace wall. The rates of mass loss of furnaces with W and Pd CM were about the same but greater than that of the control furnace (Fig. 2).

The main operating characteristic of graphite furnaces is not so much the failure as the analytical lifetime [7]. If the absorption signal intensity drops below a certain limit, then the instrument must be recalibrated or replaced by a new furnace. This entails a work stoppage and, as a result, addition lost time. Therefore, not only the wear resistance of ETAAS graphite furnaces must be considered but also the atomization signal must be routinely monitored (Fig. 3).

The furnace wall becomes more porous because of degradation of the PGC and loss of amorphous graphite at high temperatures. A part of the analyte migrates out of the furnace through pores so that the signal intensity decreases gradually. This trend is observed in any case although there are nuances.

The analytical parameters of Ag signals changed little for three fourths of all measurements until the unmodified furnace finally failed (Fig. 3a). The decreased furnace mass caused only a shift of the start of Ag atomization from measurement to measurement due to the temperature increase that was typical of easily atomized elements [8]. The W-modified furnace

TABLE 1. Visual Changes of Graphite Furnaces Resulting from Degradation in the Presence of W, Zr, and Pd Modifiers

Number of cycles	Modifier			
	None	W	Zr	Pd
0	standard new furnace (Fig. 1a)			
20	no visual changes (except insignificant damage of the SIH PGC of the Zr-modified furnace)			
40	no visual changes	destruction of the PGC around the SIH starts, no other visible changes		
60	first visible changes	SIH expands, no other visible changes	destruction of the PGC around the SIH continues, SIH diameter does not increase, no other visible changes	destruction near the SIH continues, PGC opposite the gap between graphite bushings holding the furnace (henceforth gap) changes noticeably; point corrosion of the PGC appears on the outer furnace surface
80	changes barely noticeable	SIH expands due to EG heating between inner and outer PGC layers, other furnace parts remain intact	EG exposed around the SIH, hole retains initial diameter due to furnace inner surface; destruction of the outer PGC begins (Fig. 1b)	slight SIH expansion due to destruction of furnace material (both PGC and EG); PGC opposite the gap changes; damaged points greater on the furnace surface (Fig. 1c)
120	PGC noticeably destroyed: more extensively in the analytical zone and on the furnace surface inserted into the graphite bushing	burning of SIH EG accelerates	SIH increases; signs of PGC corrosion along the analytical zone edges noticeable (Fig. 1d)	SIH increases; dark ring forms opposite the gap; total number of PGC damaged points grows; furnace part inserted into graphite bushing wears more rapidly (Fig. 1e)
120	further wear in the noted furnace regions	SIH doubles in size, PGC destruction in analytical region noticeable	destruction around SIH and analytical zone appears as pits with white deposit inside and bluish colors along the edges; PGC clearly corroded (Fig. 1f)	furnace material losses around the SIH of increased diameter; vibrant ring of markings opposite gap, traces of wear along the whole furnace surface (Fig. 1g)
189	further wear in the indicated regions	SIH increases to Ø4.0 mm because of EG destruction between PGC layers; outer PGC of furnace wall damaged	SIH not wider but wall perforated in places; persistent interference makes further measurements impossible (Fig. 1h)	SIH diameter continues to grow; outer PGC near SIH half destroyed; dark ring opposite gap changes little; signs of furnace overheating around SIH (graphite crystals)
203	destruction around SIH noticeable	SIH increases to Ø4.5–5.0 mm, sublimed graphite crystals appear; persistent noise interferes with further measurements (Fig. 1i)	–	destruction of outer PGC and furnace SIH in places described above accelerates (Fig. 1j)
233	PGC degradation of the furnace part surrounded by the bushing and destruction of material around SIH progress	–	–	furnace buckles; outer PGC disappears at SIH and wall disintegrates; clear signs of graphite sublimation (Fig. 1k)
389	furnace fails (sublimed graphite crystallizes around SIH, graphite in analytical zone changes color) (Fig. 1k and 1l)	–	–	–

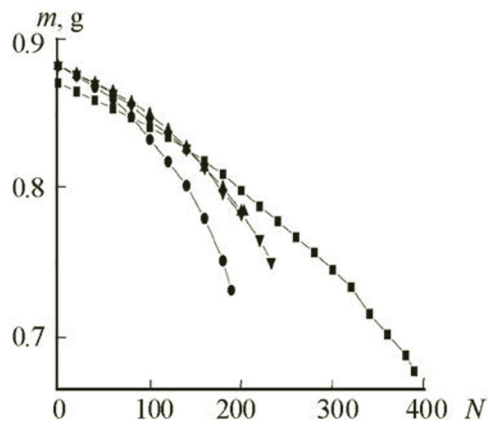


Fig. 2. Dependence of furnace mass (m) on number of cycles (N); unmodified furnace (■) and W- (▲), Zr- (●), and Pd-modified furnaces (▼).

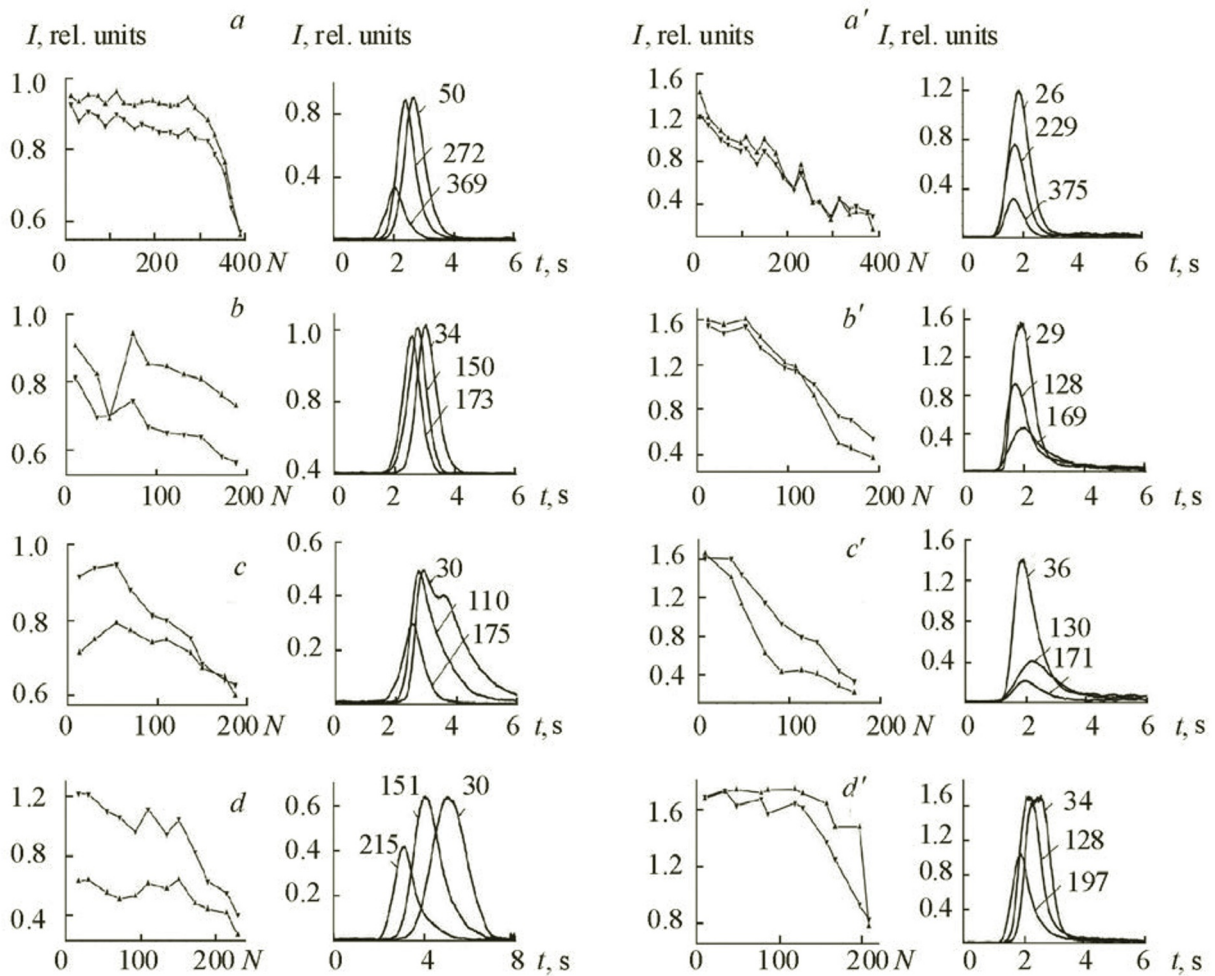


Fig. 3. Dependences of signal intensity of Ag (a–d) and Cu (a'–d') on number of cycles (N) (▲, peak maximum; ▼, integrated area) and on time (t) (numbers are ordinal numbers of cycles) for unmodified furnace (a, a') and W- (b, b'), Zr- (c, c'), and Pd-modified furnaces (d, d').

failed prematurely because of damage at the site of anomalous SIH expansion without exhausting the potential lifetime, i.e., the inner PGC persisted. This explained the slight difference in the signals at the start and end of the series of measurements. The integral peak areas were comparable to each other for the unmodified and W-modified (Na_2WO_4) furnaces.

Ag and Zr, in contrast to W, formed metallic compounds [20]. Signals with more than one peak could be observed for the intermetallides [21]. A similar situation occurred in our instance at the start of furnace operation. This in combination with the ability of Zr to penetrate at high temperatures and remain in refractory compounds in the furnace graphite wall caused tailing of the right slope of the absorption signal [22], i.e., Ag atoms held in the pores could form an independent second peak or shift the signal maximum to higher temperatures relative to the analogous signals for a surface unmodified by zirconyl nitrate if the peaks overlapped. The start of atomization and intensity maximum of the first Ag peak coincided over time with those for the W modifier. The lowest signal intensity could be explained on one hand by distribution of integral area between two peaks and, on the other, accelerated extensive furnace wear stimulated by modifier Zr component.

Pd modifier added to the sample caused a predictably greater shift of Ag signals to higher temperatures. The delayed start of atomization could be caused by the formation of clusters of Ag and Pd atoms [23]. However, the increased furnace heating temperature during wear [8] probably facilitated accelerated destruction of clusters and led over time to a gradually decreased shift that was still greater than that in the presence of the other CM.

The integrated absorption of Cu during furnace degradation with and without the various CM decreased much more than that of Ag. The start of Cu atomization remained constant. The exception was the Pd CM, addition of which to the sample led to a slight shift of the start of Cu atomization to higher temperature, like for Ag but less pronounced (Fig. 3b). Like for Ag, Cu atoms were situated among a predominant number of Pd atoms. Pd reacted first with active centers so that Pd and Cu were atomized simultaneously after the clusters were destroyed, even at high temperatures. The difference in the start of atomization of Cu and Ag could be explained by the smaller difference in the melting points of Cu and Pd as compared to Ag and Pd.

Conclusions. A general trend of decreasing integrated peak area and maximum of the analytical signals was observed as the furnace degraded. The time of the start of atomization shifted toward the origin. Several features allowed characteristics of the selected analytes or modifiers to be identified. For example, the Ag signal maxima drifted clearly from measurement to measurement toward the origin while those of Cu shifted insignificantly. The signals before and after W modification differed least of all. Relatively weak signals that often had more than one peak were obtained after Zr modification. The latest start of atomization occurred after Pd modification.

Many different factors including the sample volume and presence of compounds capable of reacting with the furnace wall material affected degradation of the atomizer furnace. Both factors became more significant after addition of a modifier. This could enhance accelerated destruction of the PGC, change the analytical signal parameters, and led to earlier failure of the furnace.

Current measurement methods assume *a priori* the use of modifiers regardless of the need to use them in each actual instance. However, modifiers apparently accelerate wear of graphite furnaces besides fulfilling their primary functions and shorten their service lives. This relates to platinum-group metals (Pd) and even more so to permanent modifiers (W, Zr).

REFERENCES

1. W. Frech, *Fresenius' J. Anal. Chem.*, **355**, 475–486 (1996).
2. U. Rohr, H. M. Ortner, G. Schlemmer, S. Weinbruch, and B. Welz, *Spectrochim. Acta, Part B*, **54**, 699–718 (1999).
3. M. A. Castro, A. J. Aller, K. Faulds, and D. Littlejohn, *J. Anal. At. Spectrom.*, **24**, 1044–1050 (2009).
4. W. Slavin, S. A. Myers, and D. C. Manning, *Anal. Chim. Acta*, **117**, 267–273 (1980).
5. H. G. C. Human, N. P. Ferreira, C. J. Rademeyer, and P. K. Faure, *Spectrochim. Acta, Part B*, **37**, 593–602 (1982).
6. H. Falk, A. Glismann, L. Bergann, G. Minkwitz, M. Schubert, and G. Skole, *Spectrochim. Acta, Part B*, **40**, 533–542 (1985).
7. H. M. Ortner, U. Rohr, G. Schlemmer, S. Weinbruch, and B. Welz, *Spectrochim. Acta, Part B*, **57**, 243–260 (2002).
8. A. N. Kulik, A. N. Bugai, Yu. V. Rogul'skii, M. I. Zakharets, and L. F. Sukhodub, *J. Eng. Phys. Thermophys.*, **80**, 159–165 (2007).
9. E. C. Lima, J. L. Brasil, and A. H. D. P. Santos, *Anal. Chim. Acta*, **484**, 233–242 (2003).
10. R. W. Fonseca, J. McNelly, and J. A. Holcombe, *Spectrochim. Acta, Part B*, **48**, 79–89 (1993).
11. Yu. V. Rogul'skii, V. Yu. Il'yashenko, and A. N. Kulik, *Zh. Prikl. Spektrosk.*, **80**, No. 6, 925–929 (2013) [Yu. V. Rogul'skiy, V. Yu. Illiashenko, and A. N. Kulik, *J. Appl. Spectrosc.*, **80**, 917–921 (2013)].

12. D. W. McKee, in: *Chemistry and Physics of Carbon*, P. L. Walker, Jr., and P. A. Thrower (Eds.), Marcel Dekker Inc., New York (1981), pp. 1–118.
13. A. B. Volynsky, E. M. Sedykh, B. Y. Spivakov, and I. Havezov, *Anal. Chim. Acta*, **174**, 173–182 (1985).
14. G. Muller-Vogt, L. Hahn, H. Muller, W. Wendl, and D. Jacquiers-Roux, *J. Anal. At. Spectrom.*, **10**, 777–783 (1995).
15. G. Muller-Vogt, F. Weigend, and W. Wendl, *Spectrochim. Acta, Part B*, **51**, 1133–1137 (1996).
16. A. B. Volynsky, *Spectrochim. Acta, Part B*, **51**, 1573–1589 (1996).
17. H. M. Ortner, E. Bulska, U. Rohr, G. Schlemmer, S. Weinbruch, and B. Welz, *Spectrochim. Acta, Part B*, **57**, 1835–1853 (2002).
18. A. B. Volynsky and R. Wennrich, *Spectrochim. Acta, Part B*, **57**, 1301–1316 (2002).
19. C. Abad, S. Florek, H. Becker-Ross, M.-D. Huang, A. G. Buzanich, M. Radtke, A. Lippitz, V.-D. Hodoroaba, T. Schmid, and H.-J. Heinrich, *J. Anal. At. Spectrom.*, **33**, 2034–2042 (2018).
20. N. P. Lyakishev (ed.), *Phase Diagrams of Binary Metal Systems* [in Russian], Mashinostroenie, Moscow (1996), Vol. 1, pp. 72, 110–112.
21. D. Rodriguez, M. A. Sanchez, and D. Rojas, *Av. Quim.*, **3**, 79–85 (2008).
22. V. I. Slaveykova, L. Lampugnani, D. L. Tsalev, L. Sabbatini, and E. DeGiglio, *Spectrochim. Acta, Part B*, **54**, 455–467 (1999).
23. A. N. Kulik, A. N. Bugai, and V. Yu. Il'yashenko, *Zh. Prikl. Spektrosk.*, **81**, No. 1, 152–158 (2014) [A. N. Kulik, A. N. Buhay, and V. Yu. Illiashenko, *J. Appl. Spectrosc.*, **81**, 151–157 (2014)].